

Modal analysis for implant stability assessment: Sensitivity of this methodology for different implant designs

Zanetti, E.M., Ciaramella, S., Cali, M., Pascoletti, G., Martorelli, M., Asero, R., Watts, D.C.

Keywords: Reverse Engineering; CAD; Finite Element Analysis; Dental Materials; Material Properties; Implant Stability; Bone Properties; Endosteal Implants; Osseointegration

Abstract

Objectives: To investigate the influence of implant design on the change in the natural frequency of bone-implant system during osseointegration by means of a modal 3D Finite Element Analysis.

Methods: Four implants by ISOMED[®], marked as A, B, C and D, were considered. Solid models were obtained by means of reverse engineering techniques. The mandibular bone geometry was build-up from a CT scan dataset through image segmentation. Each implant was virtually implanted in the mandibular bone. Two boundary condition cases were considered: mandibular branch constrained at its extreme sections (first case) and in correspondence with its outer surface (second case). Modal analyses were carried out for each boundary condition, and the first three resonance frequencies were assessed with the respective vibration modes.

Results: In the first boundary condition case, the difference between resonance frequency at whole bone maturation and resonance frequency at 10% bone maturation remained lower than 6.3% for all modes, with the exception of the third mode of vibration in the 'D' implant where this difference reached 8.3%. In the second boundary condition case, considering the first mode of vibration, 43-62% of the frequency increment was achieved at 10% osseointegration; 65-89% was achieved at 20%; 92-100% was achieved at 50% osseointegration. Flexural modes of vibration have exhibited similar behavior.

Significance: Resonance frequencies and their trends towards osseointegration level differ significantly between implant designs; tapered implants are the most sensitive to bone maturation levels. There is no

advantage in studying axial modes of vibration. Resonance frequencies are generally **not** sensitive to bone maturation level beyond 50%.

1. Introduction

As is well known, implant stability plays a major role in successful dental implantology. Primary stability (a mechanical phenomenon) is achieved when an implant has just been set in place and is related to bone quality [1], implant geometry [2], and to the surgical technique [3]. Secondary stability (a biological phenomenon) is achieved via implant osseointegration, where new bone formation leads to an increment in stiffness of the peri-implant bone, and to bone-implant interlocking.

Optimizing secondary stability requires avoiding micro-movements between the implant and the bone, since they can potentially lead to fibrous bone formation [4]. Therefore a healing period, during which the implants are unloaded, is required.

On the other hand, load application to an implant is necessary to provide stimulus for bone maturation [4]. Consequently, improved implant designs and surface treatments have led to new loading protocols, such as ‘early loading’ or ‘immediate loading’ [5]. Being true that patients are able to self-regulate masticatory load levels in relation to implant stability [6], nonetheless a quantitative measurement of implant stability prior to loading is strongly recommended.

The debate on optimal duration of the unloaded ‘healing period’ is still open and is the object of many research studies [7,8]. These have led to the conclusion that absolute indications cannot be given: since the patient bone quality, the kind of implant and the outcome of surgical technique play a fundamental role [5,9,10].

Establishing patient-specific loading protocols require a non-invasive quantitative assessment of implant stability. Vibrometry techniques could meet this aim, according to extensive data reported in the literature where numerical, experimental and clinical methods have been employed to establish the relationship between resonance frequencies and cortical bone thickness [11,12], trabecular bone density [11,13–17], implant length [12,18,19], implant diameter [20,21] and time elapsed since implant placement [16,19,22].

Clinical studies have also been performed, to gain quantitative data about the lower limit of resonance frequency providing optimal primary stability [19,23,24], or the required frequency to start implant loading [23].

However, it is not clear if, and to what extent, the sensitivity of this technique, i.e. resonance frequency variation during osseointegration, is affected by implant design. Very different implant shapes are now available (long or short; cylindrical or tapered), with different threads (single or double thread; short or large pitch, etc), and the most efficient vibration mode - the mode undergoing the highest frequency variation during osseointegration - might differ amongst implant designs.

The aim of the present study was to assess the influence of implant design on the resonance frequency variation during osseointegration, using Resonance Frequency Analysis (RFA). Details concerning the experimental set up and the boundary conditions of bone were also investigated, since they can have a considerable influence or even completely mask the osseointegration effect.

2. Materials and Methods

Modern CAD–FEM (Computer Aided Design and Finite Element Method) methodologies have been extensively used in biomedical investigations for characterizing biomechanical responses in dental applications [25–30].

Starting from these methodologies, four implants from the same manufacturer (ISOMED[®] Dental Implant, Italy) were considered and analyzed to investigate the influence of implant geometrical factors, such as shape and thread pitch, on the change of the natural frequency (i.e. resonance frequency) of bone-implant system during osseointegration.

These implants were designated as: A (cylindrical implant with internal hexagon connection TIC-10), B (conical implant with inside hexagon connection and medium thread TICc-10 BL), C (conical transmucous implant with internal hexagon connection and double thread TVI5-3-Tr-PLUS) and D (conical implant with internal hexagon connection and progressive thread PROGRESSIVE 5-10). The geometrical features of these implants are shown in Fig. 1.

2.1. Generation of solid models

Solid models of ISOMED[®] Dental implants were obtained by means of reverse engineering techniques [10]: the outer shape was digitised by a laser scanner: CAM2 Edge SCANARM HD - FARO (accuracy $\pm 25 \mu\text{m}$). Point clouds were imported into Geomagic Studio[®] software, where 3D tessellated surfaces were created, and sharp edges and cross section curves were obtained through feature detection algorithms [31]. Finally, the implant parametric 3D CAD model was created using SolidWorks[®] software ver. 2017 (SolidWorks Corporation, Concord, MA, USA).

The mandibular bone geometry was established using micro-CT scan images. Image data sets were processed using Mimics[®] software by Materialise. CAD 3D volume reconstruction was performed using Rhinoceros[®] software by Robert McNeel & Associates. The geometry was subsequently sectioned to obtain a 30 mm long portion (Fig. 2).

Each implant was virtually placed in the mandibular bone volume. Boolean operations were carried out to ensure the congruence of interfacial boundaries of the implant and bone.

The transverse mandibular section, shown in Fig. 2, consist of four distinct areas: an outer shell of cortical bone with 1.2 mm thickness in the coronal area, an inner volume of trabecular bone and two interfacial volumes. The interfacial volumes extended up to 1 mm external to the implant thread [22] and represented the cortical and trabecular bone regions, respectively, affected by implant placement and whose properties were going to change, as a result of progressive implant osseointegration [17].

Implant models were placed in a coordinate system, where the 1-axis and 2-axis were chosen for the bucco-lingual direction and mesio-distal direction, respectively, while the 3-axis was oriented upwards (Fig. 2a).

2.2. Numerical simulation

Bone remodeling was related to biomechanical responses by means of a modal three-dimensional Finite Element (FE) Analysis using ANSYS[®] v. 17.0.

In total, four different FE models were created and analysed. ANSYS software was used to mesh bone-implant system components. All volumes were discretized by 10-node tetrahedral elements TET10 with a global size ranging from 6.0×10^{-5} mm to 0.5 mm. The total number of elements was equal to about 190,000 with approximately 320,000 nodes. To minimize the mesh-dependent results, due to smaller curvatures and notch effects, mesh refinement techniques were used.

Mechanical properties assigned to each material are reported in Table 1, where the k parameter was used to simulate the variation of bone mechanical properties during osseointegration. For example, $k = 0.5$ when the bone, during its maturation, has reached 50% of its mechanical properties at full maturation. For the density at both trabecular and cortical bone interface volumes, the $k^{1/3}$ parameter was used, according to [32]. Both cortical and trabecular bones were modelled as transversely isotropic and fully characterized by four independent elastic moduli: E_1 , E_3 , ν_{12} , ν_{13} and the direction of main orthotropy axes, as deduced from literature [2].

Two extreme boundary conditions were considered: in the first case, the mandibular branch was fully constrained in correspondence with its extreme sections; in the second case, it was fully constrained on its outer surface. The second boundary condition is not physiologic. However it was simulated because the actual condition lies approximately in the middle.

A modal analysis was carried out for each boundary condition, and the first three resonance frequencies were measured with the respective vibration modes. The resonance frequencies represent natural vibration frequencies of a structure when it is moved from its stationary conditions (like a plucked string); they are related to structure stiffness, mass distribution, and boundary conditions. Finite element programs are able to calculate the value of resonance frequencies once stiffness matrix, mass matrix and boundary conditions are defined. Structures can have more than one mode of vibration, corresponding to different deformed shapes: for example a truss can bend on two planes or it can undergo torsion; consequently more than one resonance frequencies are calculated, and they are usually sorted in an ascending order.

3. Results

In this section, the change in the natural frequency *versus* osseointegration level, for different implant designs, was reported and analysed.

Fig. 3 depicts the first three modal frequencies trends for the first boundary condition case. All curves have a similar pattern: the resonance frequency has a sharp increment when bone maturation moves from 1% to 10%; from that point on, the sensitivity of resonance frequency to bone maturation drops.

With reference to the first mode of vibration and considering the frequency difference between 100% and 1% integration as a reference, over 90% of this increment was achieved at 10% osseointegration; 94-96%

was achieved at 20%; 98-99% was achieved at 50% osseointegration. In other words, the difference between resonance frequency at whole bone maturation and resonance frequency at 10% bone maturation remained less than 6.3% for all modes, with the exception of the third mode of vibration in 'D' implant where this difference reached 8.3%.

Fig. 4 shows modal shapes for $k > 0.01$, in the first boundary conditions case, where the first vibration mode was due to bone flexion around the '3' axis; the second vibration mode was produced by bone flexion around the '1' axis, and, finally, the third vibration mode was due to bone torsion.

All implants exhibited a similar behavior, which was consistent for almost all vibration modes, with the exception of the 'D' implant where implant displacements relative to bone were of greater significance. In more detail: model 'A' was the stiffest one, producing higher resonance frequencies, model 'D' was the most deformable, and model 'B' and 'C' lay in between. Differences in resonance frequency between models 'A' and 'D' reached 24% (second mode) and were equal to 22% considering the first mode; the last one is the reference mode for usual devices [18].

A further boundary condition (second case) was studied, as detailed in the previous paragraph, where the mandible outer surface was totally constrained with the aim of reducing mandibular bone deformation and giving more emphasis to implant displacement within the bone.

The pattern of frequency versus osseointegration level (Fig. 5) was still non-linear, but more gradual than in Fig. 3. With reference to the first mode of vibration and considering the frequency difference between 100% and 1% integration as a reference, 43-62% of this increment was achieved at 10% osseointegration; 65-89% was achieved at 20%; 92-100% was achieved at 50% osseointegration. In more detail: the 'C' implant model did not produce significantly different results when osseointegration proceeded from 50% to 100% osseointegration. The 'D' implant model allowed the most accurate estimate of osseointegration from the resonance frequency. 'A' and 'B' implants delivered similar outcomes.

The modes of vibration were now completely different, since implant displacements within bone implants now played a major role (Fig. 6). In more detail: the first modal shape was a rotation of the implant around '2' axis; the second was a rotation of the implant around '1' axis, and finally, the third modal shape was an axial 'sinking' of the implant. In this latter mode of vibration the implant behaves as if it were constrained with slide contact at interface volume of trabecular bone [33].

Considering the other modes of vibration, the second mode curves were less sensible to osseointegration beyond 50%, with the exception of 'D' curve (87% increment reached at 50% integration).

4. Discussion

According to results introduced in the previous paragraph, the modes of vibrations were heavily influenced by boundary conditions; this is a well known concept in structural mechanics, but the peculiarity of this application lies in the fact that the constraint of the mandibular bone led to greater emphasis on implant displacement within the bone rather than whole bone deformation.

In the first boundary condition case, vibration modes were produced by deformation of the mandibular bone itself, with minimum displacement of the implant relative to the bone. This is the reason why frequencies undergo only small variations after osseointegration has reached 10%. Large deformations of mandibular bone are the reason why resonance frequencies are not so sensitive to bone maturation: the boundary of the implant becomes a secondary aspect.

The implication of this finding is that the sensitivity of modal analysis to the osseointegration level differs between different implant positions on the mandible: the mandible behavior is likely to be stiffer in the anterior region (at least with reference to flexural loads) due to chin curvature, compared to its lateral branches.

Another implication is that clinical measurements should observe the mandible boundary conditions: eventual bone supports, muscle tightness, open or closed mouth. This problem might partially explain why resonance frequency patterns vary for different implant locations [18]. The predominance of mandibular deformation on implant displacement inside the bone was clearly outlined by Natali & al. in their numerical work [17].

These authors suggested the use of a cantilever mass in order to determine implant displacements within the bone among the first modal shapes. However this solution has not been implemented in currently used devices.

The second finding is that different implant shapes and threads result in a different pattern of resonance frequency *versus* osseointegration level. In more detail: tapered implants with high taper slope ('C' model in the present paper) are more critical because resonance frequencies do not show significant variation when

osseointegration is beyond 50%. By contrast, the 'D' model with its large pitch has proven to be the most sensitive to osseointegration level.

Finally, no significant benefit is gained by following the second or third mode of vibration; on the contrary, these modes demonstrated reduced sensitivity to osseointegration level.

As a general rule, modal analysis methods provide an accurate estimation of the osseointegration process in the very initial phase, and they give fair indications when the osseointegration level is beyond 50%, or even lower in those areas of the mandible which undergo large displacement. This finding agrees with results obtained by Li and coworkers through a numerical model where also bone remodeling has been simulated [16].

Optimisation of modal frequency analysis as a clinical tool to evaluate bone integration requires establishment of a repeatable and detailed protocol to constrain the mandibular bone by means of specific supports and clamps to be placed in the adjacent teeth to keep muscles tight while leaving the mouth partially opened.

Numerical models like those developed here and in previous work [25–30] can provide a useful tool to understand experimental results and to optimize the measurement protocol. These models can be further improved simulating bone maturation: a simplified remodeling law has been here assumed where mechanical properties are uniform in the cylinder surrounding the bone implant, while more complex behavior could be simulated, calculating bone remodeling in relation to bone loads [16], or even transport phenomena governing bone metabolism through multiphysical models [34].

Conclusions

The following conclusions were drawn:

1. Resonance frequencies and their pattern towards osseointegration level are significantly different between implants having different outer shapes and thread pitches; tapered implants are the most sensitive to bone maturation levels.
2. Flexural modes of vibration on different planes exhibited similar behavior.
3. There is no advantage in studying axial modes of vibration.

4. Protocols for modal analysis on the implanted mandible would benefit from constraining the mandibular bone by means of specific supports and clamps.
5. Resonance frequencies generally are insensitive to bone maturation levels beyond 50%.

References

1. Viridi AS, Irish J, Sena K, et al. Sclerostin Antibody Treatment Improves Implant Fixation in a Model of Severe Osteoporosis. *J Bone Jt Surg*. 2015;97(2):133-140. doi:10.2106/JBJS.N.00654
2. Cali M, Zanetti EM, Oliveri SM, et al. Influence of thread shape and inclination on the biomechanical behaviour of plateau implant systems. *Dent Mater*. February 2018. doi:10.1016/j.dental.2018.01.012
3. Heo D, Heo Y-K, Lee J-H, Lee J-J, Kim B. Comparison Between Cortical Drill and Cortical Tap and Their Influence on Primary Stability of Macro-Thread Tapered Implant in Thin Crestal Cortical Bone and Low-Density Bone. *Implant Dent*. 2017;26(5):711-717. doi:10.1097/ID.0000000000000614
4. Duyck J, Vandamme K. The effect of loading on peri-implant bone: a critical review of the literature. *J Oral Rehabil*. 2014;41(10):783-794. doi:10.1111/joor.12195
5. Al-Sawai A-A, Labib H. Success of immediate loading implants compared to conventionally-loaded implants: a literature review. *J Investig Clin Dent*. 2016;7(3):217-224. doi:10.1111/jicd.12152
6. Menicucci G, Ceruti P, Barabino E, Screti A, Bignardi C, Preti G. A preliminary in vivo trial of load transfer in mandibular implant-retained overdentures anchored in 2 different ways: allowing and counteracting free rotation. *Int J Prosthodont*. 19(6):574-576.
7. Hong DGK, Oh J. Recent advances in dental implants. *Maxillofac Plast Reconstr Surg*. 2017;39(1):33. doi:10.1186/s40902-017-0132-2
8. Schimmel M, Srinivasan M, Herrmann FR, Müller F. Loading protocols for implant-supported overdentures in the edentulous jaw: a systematic review and meta-analysis. *Int J Oral Maxillofac Implants*. 2014;29 Suppl:271-286. <http://www.ncbi.nlm.nih.gov/pubmed/24660203>. Accessed February 7, 2018.
9. Chung S, McCullagh A, Irinakis T. Immediate Loading in the Maxillary Arch: Evidence-Based Guidelines to Improve Success Rates: A Review. *J Oral Implantol*. 2011;37(5):610-621. doi:10.1563/AAID-D-JOI-10-00058.1

10. Papaspyridakos P, Chen C-J, Chuang S-K, Weber H-P. Implant loading protocols for edentulous patients with fixed prostheses: a systematic review and meta-analysis. *Int J Oral Maxillofac Implants*. 2014;29 Suppl:256-270. <http://www.ncbi.nlm.nih.gov/pubmed/24660202>. Accessed February 7, 2018.
11. Huang H-M, Lee S-Y, Yeh C-Y, Lin C-T. Resonance frequency assessment of dental implant stability with various bone qualities: a numerical approach. *Clin Oral Implants Res*. 2002;13(1):65-74. doi:10.1034/J.1600-0501.2002.130108.X
12. Miyamoto I, Tsuboi Y, Wada E, Suwa H, Iizuka T. Influence of cortical bone thickness and implant length on implant stability at the time of surgery—clinical, prospective, biomechanical, and imaging study. *Bone*. 2005;37(6):776-780. doi:10.1016/J.BONE.2005.06.019
13. (OFFA) OF for A. Hip Dysplasia Statistics. Hip Dysplasia by Breed and Rank. Trends in Hip Dysplasia (selected breeds). http://www.offa.org/stats_hip.html?view=2. Accessed May 6, 2016.
14. Friberg B, Sennerby L, Meredith N, Lekholm U. A comparison between cutting torque and resonance frequency measurements of maxillary implants. *Int J Oral Maxillofac Surg*. 1999;28(4):297-303. doi:10.1016/S0901-5027(99)80163-5
15. Farré-Pagès N, Augé-Castro ML, Alaejos-Algarra F, Mareque-Bueno J, Ferrés-Padró E, Hernández-Alfaro F. Relation between bone density and primary implant stability. *Med Oral Patol Oral Cir Bucal*. 2011;16(1):62-67. doi:10.4317/medoral.16.e62
16. Li W, Lin D, Rungsiyakull C, Zhou S, Swain M, Li Q. Finite element based bone remodeling and resonance frequency analysis for osseointegration assessment of dental implants. *Finite Elem Anal Des*. 2011;47(8):898-905. doi:10.1016/j.finel.2011.03.009
17. Natali AN, Pavan PG, Schileo E, Williams KR. A numerical approach to resonance frequency analysis for the investigation of oral implant osseointegration. *J Oral Rehabil*. 2006;33(9):674-681. doi:10.1111/j.1365-2842.2006.01610.x
18. Sjöström M, Sennerby L, Nilson H, Lundgren S. Reconstruction of the atrophic edentulous maxilla with free iliac crest grafts and implants: A 3-year report of a prospective clinical study. *Clin Implant Dent Relat Res*. 2007;9(1):46-59. doi:10.1111/j.1708-8208.2007.00034.x
19. Sennerby L, Meredith N. Implant stability measurements using resonance frequency analysis:

- biological and biomechanical aspects and clinical implications. *Periodontol 2000*. 2008;47(1):51-66. doi:10.1111/j.1600-0757.2008.00267.x
20. Simunek A, Strnad J, Kopecka D, et al. Changes in stability after healing of immediately loaded dental implants. *Int J Oral Maxillofac Implants*. 2010;25(6):1085-1092. <http://www.ncbi.nlm.nih.gov/pubmed/21197483>.
 21. Huwiler MA, Pjetursson BE, Bosshardt DD, Salvi GE, Lang NP. Resonance frequency analysis in relation to jawbone characteristics and during early healing of implant installation. *Clin Oral Implants Res*. 2007;18(3):275-280. doi:10.1111/j.1600-0501.2007.01336.x
 22. Glauser R, Sennerby L, Meredith N, et al. Resonance frequency analysis of implants subjected to immediate or early functional occlusal loading. Successful vs. failing implants. *Clin Oral Implants Res*. 2004;15(4):428-434. doi:10.1111/j.1600-0501.2004.01036.x
 23. Baltayan S, Pi-Anfruns J, Aghaloo T, Moy PK. The predictive value of resonance frequency analysis measurements in the surgical placement and loading of endosseous implants. *J Oral Maxillofac Surg*. 2016;74(6):1145-1152. doi:10.1016/j.joms.2016.01.048
 24. Nedir R, Bischof M, Szmukler-Moncler S, Bernard JP, Samson J. Predicting osseointegration by means of implant primary stability: A resonance-frequency analysis study with delayed and immediately loaded ITI SLA implants. *Clin Oral Implants Res*. 2004;15(5):520-528. doi:10.1111/j.1600-0501.2004.01059.x
 25. Giordano M, Ausiello P, Martorelli M. Accuracy evaluation of surgical guides in implant dentistry by non-contact reverse engineering techniques. *Dent Mater*. 2012;28(9):e178-85. doi:10.1016/j.dental.2012.06.006
 26. Ausiello P, Ciaramella S, Garcia-Godoy F, et al. The effects of cavity-margin-angles and bolus stiffness on the mechanical behavior of indirect resin composite class II restorations. *Dent Mater*. 2017;33(1):e39-e47. doi:10.1016/j.dental.2016.11.002
 27. Ausiello P, Ciaramella S, Fabianelli A, et al. Mechanical behavior of bulk direct composite versus block composite and lithium disilicate indirect Class II restorations by CAD-FEM modeling. *Dent Mater*. 2017;33(6):690-701. doi:10.1016/j.dental.2017.03.014
 28. Ausiello P, Ciaramella S, Garcia-Godoy F, Martorelli M, Sorrentino R, Gloria A. Stress distribution

of bulk-fill resin composite in class II restorations. *Am J Dent*. 2017;30(4):227-232.

29. Ausiello P, Ciaramella S, Martorelli M, Lanzotti A, Gloria A, Watts DC. CAD-FE modeling and analysis of class II restorations incorporating resin-composite, glass ionomer and glass ceramic materials. *Dent Mater*. 2017;33(12):1456-1465. doi:10.1016/j.dental.2017.10.010
30. Ausiello P, Ciaramella S, Martorelli M, et al. Mechanical behavior of endodontically restored canine teeth: Effects of ferrule, post material and shape. *Dent Mater*. 2017;33(12):1466-1472. doi:10.1016/j.dental.2017.10.009
31. Cali M, Oliveri SM, Fatuzzo G, Sequenzia G. Error control in UAV image acquisitions for 3D reconstruction of extensive architectures. In: Springer, Cham; 2017:1209-1219. doi:10.1007/978-3-319-45781-9_121
32. Carter DR, Hayes WC. The Compressive Behavior Porous of Bone Structure as a Two-Phase Porous Structure. *J Bone Jt Surg*. 1977;59(7):954-962. doi:10.1007/978-1-4471-5451-8_116
33. Cali M, Oliveri SM, Sequenzia G, Fatuzzo G. An effective model for the sliding contact forces in a multibody environment. *Lect Notes Mech Eng*. 2017:675-685. doi:10.1007/978-3-319-45781-9_68
34. De Napoli IE, Zanetti EM, Fragomeni G, Giuzio E, Audenino AL, Catapano G. Transport modeling of convection-enhanced hollow fiber membrane bioreactors for therapeutic applications. *J Memb Sci*. 2014;471:347-361. doi:10.1016/j.memsci.2014.08.026

Figures and figure captions

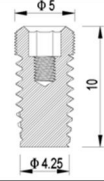

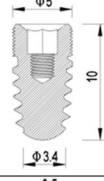

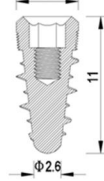

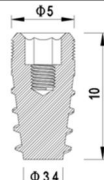

Implant type	Screw Section Design	Render
Implant "A" Cylindrical implant with internal hexagon		
Implant "B" Conical implant with internal hexagon and medium thread		
Implant "C" Conical PLUS implant with internal hexagon and double thread transmucosi		
Implant "D" Conical implant with internal hexagon and double thread progressive		

Fig. 1 – ISOMED implants: geometric characteristics.

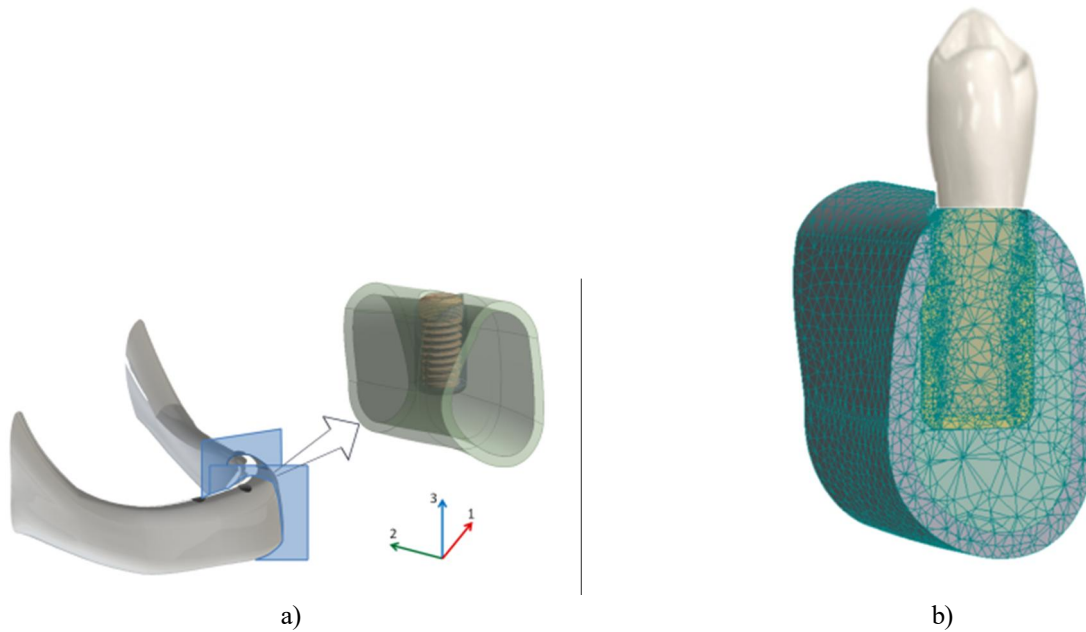


Fig. 2 – (a) Bone-implant system: (a) geometry and coordinate system; (b) FE model.

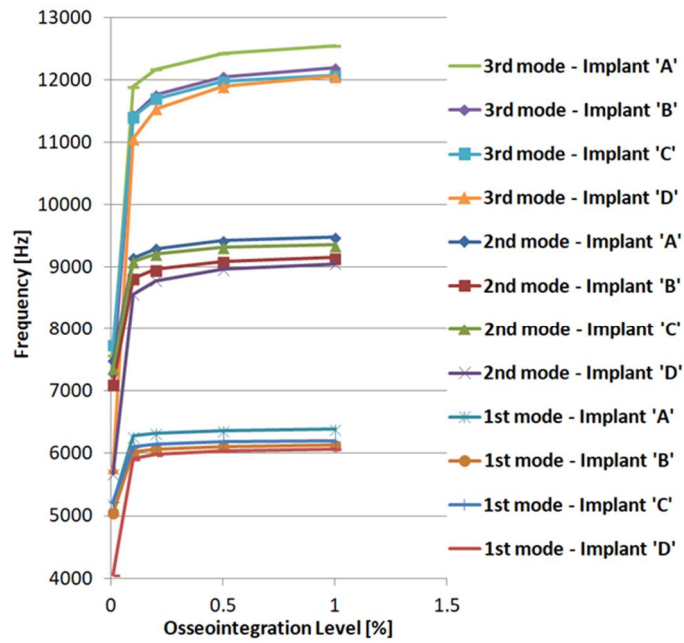


Fig. 3 – Modal frequencies versus osseointegration level for different implant designs – end constrains.

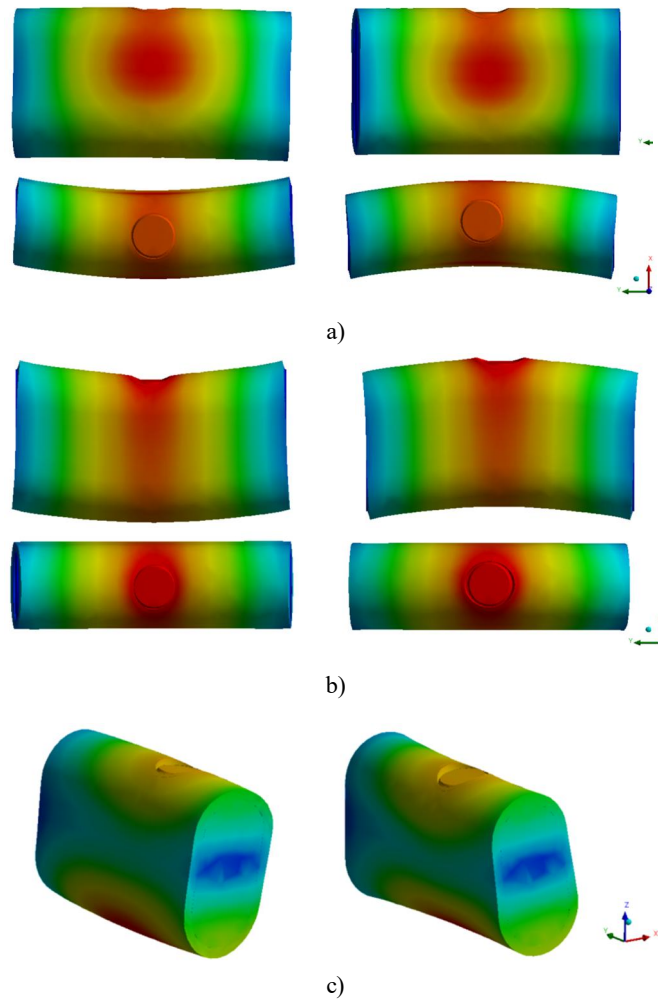


Fig. 4 - Modal shapes for the mandible constrained at its end and $k > 0.1$: (a) 1st mode (flexion around '3' axis); (b) 2nd mode (flexion around '1' axis); (c) 3rd mode (torsion)

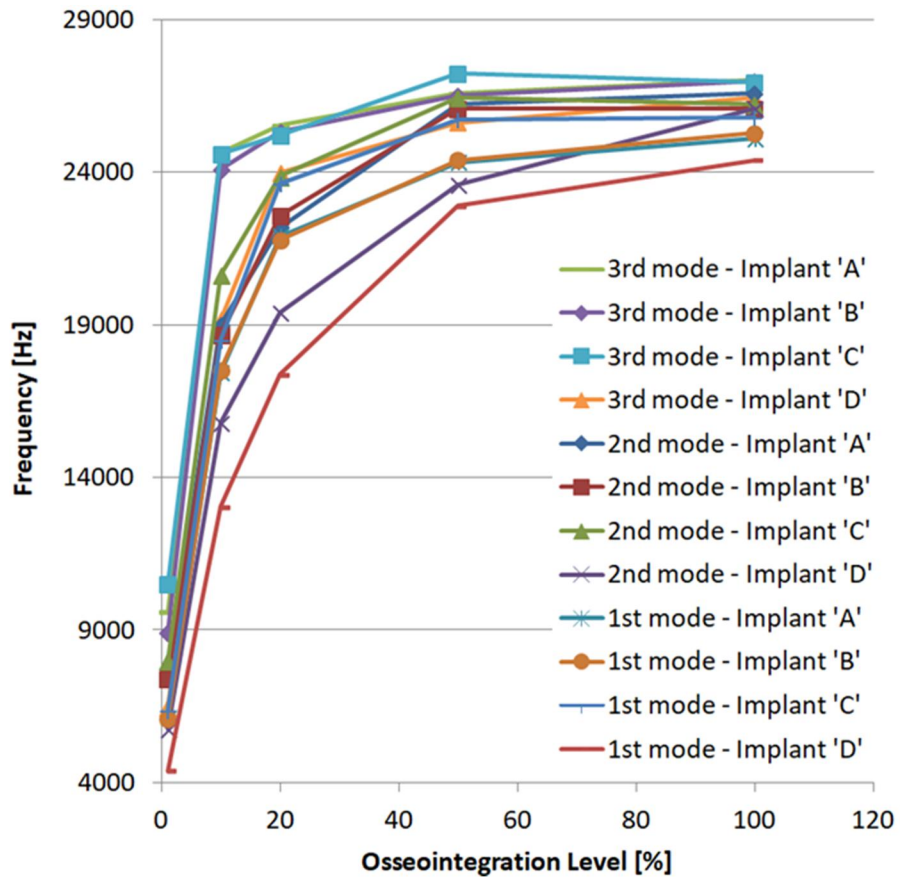
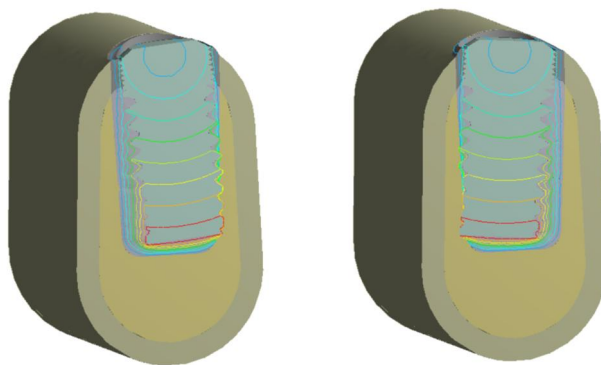
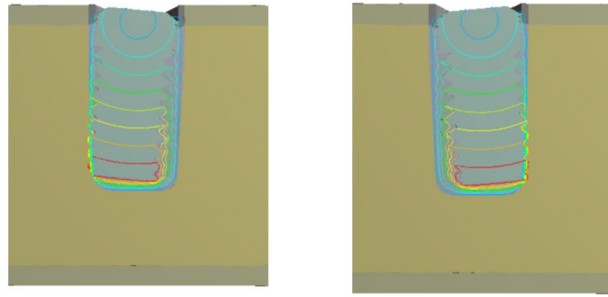


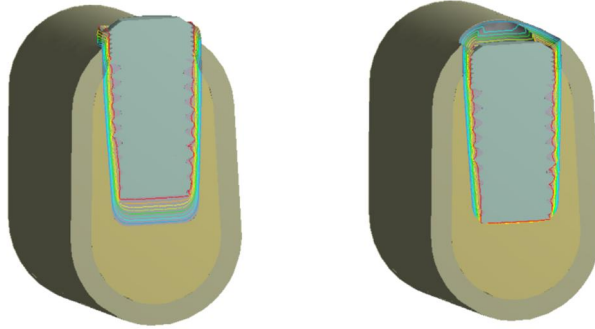
Fig. 5 - Modal frequencies versus osseointegration level for different implant designs – full mandibular-+ constraints



a)



b)



c)

Fig. 6 - Modal shapes for the fully constrained mandible: (a) 1st mode (rotation around '2' axis); (b) 2nd mode (rotation around '1' axis); (c) 3rd mode (axial displacement).